Neural Network Adaptive Iterative Learning Control for Strict-Feedback Unknown Delay Systems Against Input Saturation

Mouquan Shen, *Member, IEEE*, Zihao Wang, Song Zhu, Xudong Zhao, Guangdeng Zong, *Senior Member, IEEE*, and Qing-Guo Wang

***Abstract*— Neural network adaptive iterative learning control (ILC) is developed in this article to treat strict-feedback nonlinear systems with unknown state delays and input saturation. These delays are treated by constructing the Lyapunov–Krasovskii (L–K) functions for each subsystem. A command filter is employed to avoid the derivative explosion caused by continuous differentiation of the virtual controller. Corresponding auxiliary systems are designed and integrated into the backstepping procedure to compensate input saturation and the unimplemented part of the filter. Hyperbolic tangent functions and radial basis function neural networks (RBF NNs) are employed to treat singularity and related unknown terms, respectively. The convergence of the resultant strict-feedback systems is ensured in the framework of composite energy function (CEF). Finally, a simulation example is adopted to substantiate the validity of the proposed algorithm.**

***Index Terms*— Composite energy function (CEF), input saturation, iterative learning control (ILC), strict-feedback systems.**

Received 6 March 2024; revised 27 June 2024; accepted 28 August 2024. This work was supported in part by the National Natural Science Foundation of China under Grant 62173177, Grant 62273254, Grant 62373060, and Grant U21A20477; in part by the Introduction Plan for High-End Foreign Experts under Grant G2023014108L; in part by the National Key Research and Development Program of China under Grant 2023YFB4706800; in part by the Natural Science Foundation of Tianjin under Grant 23JCYBJC00380; and in part by the Financial Support of Beijing Normal University (BNU) Seed Fund and BNU-HKBU (Hong Kong Baptist University) United International College (UIC) Startup Fund, China, under Grant R72021115. *(Corresponding author: Mouquan Shen.)*

Mouquan Shen is with the College of Electrical Engineering and Control Science, Nanjing Tech University, Nanjing 211816, China (e-mail: shenmouquan@njtech.edu.cn).

Zihao Wang is with the School of Mechanical and Power Engineering, Nanjing Tech University, Nanjing 211816, China (e-mail: wangzihao@njtech.edu.cn).

Song Zhu is with the School of Mathematics, China University of Mining and Technology, Xuzhou 221116, China (e-mail: songzhu82@gmail.com).

Xudong Zhao is with the Faculty of Electronic Information and Electrical Engineering, Dalian University of Technology, Dalian 116024, China (e-mail: xdzhaohit@gmail.com).

Guangdeng Zong is with the School of Control Science and Engineering, Tiangong University, Tianjin 300387, China, and also with the College of Machinery and Automation, Weifang University, Weifang 261061, China (e-mail: lovelyletian@gmail.com).

Qing-Guo Wang is with the Institute of Artificial Intelligence and Future Networks, Beijing Normal University, Zhuhai 519087, China, also with Guangdong Key Laboratory of AI and Multi-Modal Data Processing, BNU-HKBU United International College, Zhuhai 519087, China, and also with the Faculty of Engineering and the Built Environment, Institute for Intelligent Systems, University of Johannesburg, Johannesburg 2006, South Africa (e-mail: wangq@uj.ac.za).

Digital Object Identifier 10.1109/TNNLS.2024.3452721

I. Introduction

ITERATIVE learning control (ILC) aims to achieve reference trajectory tracking through repeated tasks [1]. Due to its ease of implementation and excellent tracking performance, ILC has generated a series of applications, such as robotic arms, high-speed trains, quadrotor UAV, ventricular assist devices, multizone HVAC [2], [3], [4], [5], [6], [7], and so on. Simultaneously, captivating findings have surfaced concerning the theory of ILC [8], [9], [10], [11], [12], [13], [14], [15], [16]. Yu et al. [8] present a distributed adaptive ILC (DAILC) to tackle unknown dynamics and iteration-varying communication topologies. Meng and Zhang [9] present a method to transform general multi-input multi-output (MIMO) ILC into equivalent ILC. Uchiyama [10] investigates an approach for acquiring the desired trajectory function. A data-driven indirect ILC is introduced in [14] by integrating iterative dynamic linearization and inner-loop proportional–integral–derivative feedback. Chen and Hua [15] exhibit an iterative learning-based fault-tolerant control for uncertain multiagent systems with actuator faults. An event-triggered ILC is presented by [16] to alleviate computational burden and achieve cooperation among multiple subway trains. The systems mentioned above contain various types of unknown uncertainties and disturbances, which are treated by radial basis function neural networks (RBF NNs). An AILC algorithm combined with RBF NNs is presented for a class of subway trains [17]. Sun et al. [18] propose an AILC strategy with dead-zone modifications to handle arbitrary initial shifts. An RBF NN-based ILC scheme is built in [19] via a dynamic linearization approach.

Strict-feedback systems, as a type of high-order systems, have been widely discussed in recent years [20], [21], [22], [23], [24], [25], [26], [27]. To be specific, [21] exploits a predictive performance control for real-time online estimation of target trajectory. A stochastic adaptive dual domination is exploited in [23] in terms of an adaptive gain state observer to handle unknown state and sensor uncertainty. Yin et al. [24] propose a novel adaptive fuzzy control scheme to address the adverse effects of system uncertainties and disturbances. In conjunction with event-triggered idea, [25] establishes a control method using intermittent state feedback. Li et al. [27] propose an adaptive prescribed performance control

scheme for MIMO strict-feedback systems without initial error verification.

Note that the abovementioned works are conducted without state delays. In fact, these delays lead to greater complexity in control tasks, especially when they are unknown [28]. Consequently, ILC strategies are explored in [29] and [30] for unknown delays strict-feedback systems and nonrepetitive nonlinear systems, respectively. Wei et al. [31] present an ILC method for high-order systems with input dead zone, unknown state delays, and disturbances. However, the aforementioned works do not take into account input saturation, which causes the difficulties in controller design and affects system stability [32]. Therefore, remarkable achievements have emerged [2], [33], [34], [35], [36], [37], [38], [39], [40], [41], [42]. Xu et al. [33] deliver an ILC scheme for uncertain nonlinear systems with input saturation by means of a composite energy function (CEF). Wei et al. [34] introduce an additive-state-decomposition-based ILC method for nonminimum phase nonlinear systems. A feedback ILC method is developed in [35] to deal with large control input. Meng and He [2] exploit a dual-loop ILC law composed of a learning part and a feedback term. Pakshin et al. [36] investigate a vector Lyapunov function-based ILC against input saturation. An error tracking method is built in [37] to cope with the initial error of the strict-feedback systems. A nonlinear filter-based AILC is adjusted in [38] for strict-feedback systems with input saturation. Bu et al. [39] put forward a guaranteed cost robust control for uncertain 2-D systems. Li and Wei [40] present an optimal synchronization control for saturated multiagent systems through a nonzero-sum game. Chu et al. [41] construct a concensus tracking scheme via the low-and-high gain output feedback technique to deal with input saturation. A guaranteed performance tracking is discussed in [42] for uncertain strict-feedback systems with input saturation. Unfortunately, input saturation and unknown state delays have not been simultaneously taken into account for ILC design of strict-feedback systems.

To supply a possible treatment, this article strives to consider neural network AILC (NNAILC) for unknown delay strict-feedback systems with input saturation. Individual Lyapunov–Krasovskii (L–K) function for each subsystems is designed to compensate unknown state delays and construct virtual controller without the requirement of its continuous differentiation by means of a command filter. Saturated updating laws and differential updating laws are exploited to approximate the ideal weights and the estimation error of RBF NNs, respectively. A CEF is developed to ensure the boundedness of the tracking error and the compensation error. A comparative simulation study is executed on a single-link manipulator to validate the advantage of the proposed ILC scheme.

The reminder of the organization consists of four parts. Namely, the control system and its related assumptions are presented in Section II. Section III is devoted to the backstepping-based ILC design and convergence analysis. An illustrative example is presented in Section IV. Section V draws a conclusion.

Notations: $\mathbf{Z}_+$ denotes the set of positive integer. $\mathbf{R}^i$ is the space of all i-dimensional vectors. proj$(\cdot)$ represents the projection of a parameter. $\|\cdot\|$ denotes the Euclidean norm of a vector.

II. Problem Formulation

Consider the following strict-feedback nonlinear system:

$$\begin{cases} \dot{x}_{i,k}(\varrho) = f_i\left(x_{i,k}(\varrho-\tau_i)\right) + d_i\left(x_{i,k}(\varrho)\right) \\ \qquad\qquad + g_i\left(x_{i,k}(\varrho)\right) x_{i+1,k}(\varrho), \quad i = 1,\ldots,n-1 \\ \dot{x}_{n,k}(\varrho) = f_n\left(x_{n,k}(\varrho-\tau_n)\right) + d_n\left(x_{n,k}(\varrho)\right) \\ \qquad\qquad + g_n\left(x_{n,k}(\varrho)\right) u\left(v_k(\varrho)\right) \\ y_k(\varrho) = x_{1,k}(\varrho) \end{cases} \tag{1}$$

where $k \in \mathbf{Z}_+$ is iterative index and $\varrho \in [0, T]$ is execution time per iteration. $x_{i,k}(\varrho) \in \mathbf{R}(i = 1,\ldots,n)$ is the state at the kth iteration, and $x_{i,k}(\varrho)$ and $x_{n,k}(\varrho)$ are presented as $x_{i,k}(\varrho) = [x_{1,k}(\varrho),\ldots,x_{i,k}(\varrho)]^{\mathrm{T}} \in \mathbf{R}^i$ and $x_{n,k}(\varrho) = [x_{1,k}(\varrho),\ldots,x_{n,k}(\varrho)]^{\mathrm{T}} \in \mathbf{R}^n$, respectively. $y_k(\varrho) \in \mathbf{R}$ is system output. $g_i(\cdot)$:$\mathbf{R}^i \to \mathbf{R}$ is a known state-dependent smooth function, $f_i(\cdot)$:$\mathbf{R}^i \to \mathbf{R}$ is an unknown smooth function with time-delay states $x_{i,k}(\varrho-\tau_i) = [x_{1,k}(\varrho-\tau_1),\ldots,x_{i,k}(\varrho-\tau_i)]^{\mathrm{T}} \in \mathbf{R}^i$, and $d_i(\cdot)$:$\mathbf{R}^i \to \mathbf{R}$ is the unknown dynamic disturbance. $\tau_i \in \mathbf{R}$ is the unknown time delay. $v_k(\varrho) \in \mathbf{R}$ is the ideal control input, and $u(v_k(\varrho)) \in \mathbf{R}$ is the control input subject to saturation constraints, taking the following form:

$$\begin{aligned} u\left(v_k(\varrho)\right) &= \mathrm{proj}_u\left(v_k(\varrho)\right) \\ &= \begin{cases} u_m \mathrm{sign}\left(v_k(\varrho)\right), & |v_k(\varrho)| \geqslant u_m \\ v_k(\varrho), & |v_k(\varrho)| < u_m \end{cases} \end{aligned} \tag{2}$$

where u_m represents the input saturation boundary.

Assumption 1 [29]: The state delays are only related to the state itself and independent of the iteration numbers

$$x_{i,k_1}(\varrho) = x_{i,k_2}(\varrho), \quad \varrho \in [-\tau_i, 0] \tag{3}$$

where k_1 and k_2 represent different iteration numbers.

Assumption 2: The resetting condition is adopted; that is, $y_{1,k}(0) = y_d(0)$ for any $k \in \mathbf{Z}_+$.

Assumption 3 [20]: The desired trajectory $y_d(\varrho)$ and its first derivative $\dot{y}_d(\varrho)$ exhibit continuity, boundedness, and availability.

Assumption 4: The upper and lower bounds of function $g_i(x_{i,k}(\varrho))$ are known for $i = 1,\ldots,n$, i.e., $g_{\min} \leqslant g_i(x_{i,k}(\varrho)) \leqslant g_{\max}$.

Assumption 5: The unknown function $f_i(\cdot)$ with unknown state delays satisfies the following inequality:

$$\left|f_i\left(x_{i,k}(\varrho-\tau_i)\right)\right| \leqslant \theta_i(\varrho) \sum_{j=1}^{i} \rho_{i,j}\left(x_{j,k}(\varrho-\tau_i)\right) \tag{4}$$

where $\theta_i(\cdot)$ and $\rho_{i,j}(\cdot)$ are unknown.

Assumption 6: The unknown dynamic disturbance $d_i(x_{i,k}(\varrho))$ is bounded; i.e., $|d_i(x_{i,k}(\varrho))| \leqslant \mu_i(x_{i,k}(\varrho))$, where $\mu_i(\cdot)$ is unknown.

Remark 1: Assumption 2 serves as a prerequisite for achieving perfect tracking [29], [43], [44], [45]. Assumption 3 implies that there is no need for a priori knowledge of the full-order derivatives of the desired trajectory. Compared

with [29], Assumption 5 relaxes the constraint on $f_i(\cdot)$ to be completely unknown.

Lemma 1 [31]: For any positive constant ν and variable $\xi \in \mathbf{R}$, one has

$$\lim_{\xi \to 0} \frac{1}{\xi} \tanh^2\left(\frac{\xi}{\nu}\right) = 0. \tag{5}$$

Lemma 2 [46]: For $\forall W_i^* \in [W_i^{\min}, W_i^{\max}]$ and $\forall \text{proj}(\hat{W}_{i,k}^{\nabla}) \in [W_i^{\min}, W_i^{\max}]$, one has

$$\left(\hat{W}_{i,k}^{\nabla} - \text{proj}\left(\hat{W}_{i,k}^{\nabla}\right)\right)^{\mathrm{T}} \left(W_i^* - \text{proj}\left(\hat{W}_{i,k}^{\nabla}\right)\right) \leqslant 0.$$

Lemma 3 [29]: For the positive constant ν and $\Omega_z = \{z \| z| < 0.8814\nu\}$, if $z \notin \Omega_z$, then the following inequality holds:

$$1 - 2\tanh^2\left(\frac{z}{\nu}\right) \leqslant 0. \tag{6}$$

III. Main Results

To use the backstepping procedure, the coordinate transformation of the strict-feedback system (1) is taken as follows:

$$\begin{cases} e_{1,k} = y_{1,k} - y_d \\ e_{i,k} = x_{i,k} - \beta_{i,k}, \quad i = 2, \ldots, n \end{cases} \tag{7}$$

where $\beta_{i,k}(\varrho)$ is the output of command filter evolved as $\dot{\beta}_{i,k} = -\kappa_i(\beta_{i,k} - \alpha_{i-1,k})$, which $\alpha_{i,k}(\varrho)$ is the virtual controller for the ith subsystem and $\kappa_i > 0$ is the bandwidth parameter [29]. Moreover, $\beta_{i,k}(0) = \alpha_{i-1,k}(0)$. To overcome the impact of the unimplemented part $\beta_{i,k}(\varrho) - \alpha_{i-1,k}(\varrho)$ of the filter on system stability, an auxiliary system is constructed as follows:

$$\begin{cases} \dot{\gamma}_{1,k} = -c_1\gamma_{1,k} + g_{1,k}\left(\beta_{2,k} - \alpha_{1,k}\right) + g_{1,k}\gamma_{2,k} \\ \dot{\gamma}_{i,k} = -c_i\gamma_{i,k} + g_{i,k}\left(\beta_{i+1,k} - \alpha_{i,k}\right) + g_{i,k}\gamma_{i+1,k} \\ \qquad -g_{i-1,k}\gamma_{i-1,k}, \quad i = 2, \ldots, n-1 \\ \dot{\gamma}_{n,k} = -c_n\gamma_{n,k} - g_{n-1,k}\gamma_{n-1,k} \end{cases} \tag{8}$$

where $g_{i,k} \triangleq g_i(x_{i,k}(\varrho))$, $\gamma_{i,k}$ is the auxiliary system state, and $c_i > 0$ is the parameter to be designed.

On the other hand, input saturation is treated by the following auxiliary system:

$$\begin{cases} \dot{\delta}_{1,k} = -c_1\delta_{1,k} + g_{1,k}\delta_{2,k} \\ \dot{\delta}_{i,k} = -c_i\delta_{i,k} + g_{i,k}\delta_{i+1,k} - g_{i-1,k}\delta_{i-1,k}, \\ \qquad i = 2, \ldots, n-1 \\ \dot{\delta}_{n,k} = -c_n\delta_{n,k} - g_{n-1,k}\delta_{n-1,k} + g_{n,k}\Delta u_k \end{cases} \tag{9}$$

where $\delta_{i,k}$ is the auxiliary system state and $\Delta u_k = u(v_k) - v_k$ denotes the difference between the saturated control input and the actual control input.

Combining (8) and (9) yields the compensation error as follows:

$$z_{i,k} = e_{i,k} - \gamma_{i,k} - \delta_{i,k}, \quad i = 1, \ldots, n. \tag{10}$$

Before designing the virtual controllers and the actual controller, RBF NN is adopted to handle the unknown terms

$$\eta(X) = \Theta^{*\mathrm{T}}(\varrho)\,\Phi(X) + \varepsilon(X) \tag{11}$$

where $\eta(X)$ represents the unknown terms to be estimated, $X \in \mathbf{R}^l$ denotes the variable of the activation function, and $\varepsilon(X)$ is inherent NN approximation error satisfying $\varepsilon(X) \leqslant \bar{\varepsilon}$ with unknown constant $\bar{\varepsilon} \geqslant 0$. $\Phi(X) = [\phi_1(X), \phi_2(X), \ldots, \phi_N(X)]^{\mathrm{T}} \in \mathbf{R}^N$ is Gaussian basis function vector with $\phi_i(X) = \exp(-(\|X - a_i\|^2)/\sigma_i^2)$, $i = 1, \ldots, N$, where N denotes the number of nodes in NN, $a_i \in \mathbf{R}^l$ represents the center of the ith NN node, and $\sigma_i \in \mathbf{R}$ denotes the width of the ith NN node. $\Theta^*(\varrho)$ is ideal time-varying NN weight matrix defined as follows:

$$\Theta^* = \arg\min_{W \in \mathbf{R}^N} \left\{ \sup_{X \in \mathbf{R}^l} \left| \eta(X) - \Theta^{\mathrm{T}}\Phi(X) \right| \right\}. \tag{12}$$

Based on the backstepping method, the design of controllers is divided into n steps.

Step 1: From (1) and (7), $\dot{e}_{1,k}$ is calculated as follows:

$$\dot{e}_{1,k} = f_1\left(x_{1,k}(\varrho - \tau_1)\right) + g_{1,k}\left[\alpha_{1,k} + e_{2,k} + \left(\beta_{2,k} - \alpha_{1,k}\right)\right] + d_{1,k} - \dot{y}_d \tag{13}$$

where $d_{1,k} \triangleq d_1(x_{1,k})$.

According to (8)–(10) and (13), the derivative of $z_{1,k}$ is

$$\dot{z}_{1,k} = f_1\left(x_{1,k}(\varrho - \tau_1)\right) + g_{1,k}\left(\alpha_{1,k} + z_{2,k}\right) + c_1\gamma_{1,k} + c_1\delta_{1,k} + d_{1,k} - \dot{y}_d. \tag{14}$$

The candidate L–K functional is chosen as follows:

$$V_{1,k} = \frac{1}{2}z_{1,k}^2 + \frac{1}{2}\int_{\varrho-\tau_1}^{\varrho} \rho_{1,1}^2\left(x_{1,k}(\tau)\right) d\tau. \tag{15}$$

Calculating $\dot{V}_{1,k}$ provides

$$\dot{V}_{1,k} = z_{1,k}\left[g_{1,k}\left(z_{2,k} + \alpha_{1,k}\right) + c_1\gamma_{1,k} + c_1\delta_{1,k} - \dot{y}_d\right] + z_{1,k}f_1\left(x_{1,k}(\varrho - \tau_1)\right) + z_{1,k}d_{1,k} + \frac{1}{2}\rho_{1,1}^2\left(x_{1,k}\right) - \frac{1}{2}\rho_{1,1}^2\left(x_{1,k}(\varrho - \tau_1)\right). \tag{16}$$

According to Assumption 5, $z_{1,k}f_1(x_{1,k}(\varrho - \tau_1))$ in (16) becomes

$$z_{1,k}f_1\left(x_{1,k}(\varrho - \tau_1)\right) \leqslant \frac{1}{2}z_{1,k}^2\theta_1^2 + \frac{1}{2}\rho_{1,1}^2\left(x_{1,k}(\varrho - \tau_1)\right). \tag{17}$$

Similarly, from Assumption 6, $z_{1,k}d_{1,k}$ in (16) yields

$$z_{1,k}d_{1,k} \leqslant \frac{1}{2}z_{1,k}^2\mu_{1,k}^2 + \frac{1}{2}. \tag{18}$$

Substituting (17) and (18) into (16) gives

$$\dot{V}_{1,k} \leqslant z_{1,k}\left[g_{1,k}\left(z_{2,k} + \alpha_{1,k}\right) + c_1\gamma_{1,k} + c_1\delta_{1,k} - \dot{y}_d + \frac{1}{2}z_{1,k}\theta_1^2 + \frac{1}{2}z_{1,k}\mu_{1,k}^2\right] + \frac{1}{2}\psi_{1,k} \tag{19}$$

where $\psi_{1,k} = \rho_{1,1}^2(x_{1,k}) + 1$

Remark 2: Due to the unknown $\rho_{1,1}(x_{1,k})$, even if $(1/2)\psi_{1,k}$ is incorporated into $\dot{z}_{1,k}$ as part of $1/(2z_{1,k})\psi_{1,k}$, the controller cannot be directly designed. When $z_{1,k}$ tends to zero, the boundedness of (1) cannot be guaranteed due to singularity. Therefore, to address both singularity and uncertainty of

$(1/2)\psi_{1,k}$, Lemma 1 and RBF NNs are, respectively, adopted in the following.

Applying Lemma 1 to $(1/2)\psi_{1,k}$ gives

$$\frac{1}{2}\psi_{1,k} = \tanh^2\left(\frac{z_{1,k}}{\nu_1}\right)\psi_{1,k} + \frac{1}{2}\left[1 - 2\tanh^2\left(\frac{z_{1,k}}{\nu_1}\right)\right]\psi_{1,k} \tag{20}$$

where ν_1 is a positive constant.

Taking (20) into (19) supplies

$$\begin{aligned}\dot{V}_{1,k} \leqslant\ & z_{1,k}\Bigg[g_{1,k}\left(z_{2,k}+\alpha_{1,k}\right) + c_1\gamma_{1,k} + c_1\delta_{1,k} - \dot{y}_d \\ & + \underbrace{\frac{1}{2}z_{1,k}\theta_1^2 + \frac{1}{2}z_{1,k}\mu_{1,k}^2 + \frac{1}{z_{1,k}}\tanh^2\left(\frac{z_{1,k}}{\nu_1}\right)\psi_{1,k}}_{\eta_1}\Bigg] \\ & + \frac{1}{2}\left[1 - 2\tanh^2\left(\frac{z_{1,k}}{\nu_1}\right)\right]\psi_{1,k}.\end{aligned} \tag{21}$$

By employing RBF NNs, η_1 in (21) is approximated by

$$\eta_1 = \Theta_1^{*\mathrm{T}}\Phi_1\left(X_{1,k}\right) + \varepsilon_1\left(X_{1,k}\right) \tag{22}$$

where $X_{1,k} = [x_{1,k}, \gamma_{1,k}, \delta_{1,k}]^{\mathrm{T}}$.

Combining (21) and (22) results in

$$\begin{aligned}\dot{V}_{1,k} \leqslant\ & z_{1,k}\left[g_{1,k}\left(z_{2,k}+\alpha_{1,k}\right) + c_1\gamma_{1,k} + c_1\delta_{1,k} - \dot{y}_d\right. \\ & \left. + \Theta_1^{*\mathrm{T}}\Phi_1\left(X_{1,k}\right) + \bar{\varepsilon}_1\left(X_{1,k}\right)\right] \\ & + \frac{1}{2}\left[1 - 2\tanh^2\left(\frac{z_{1,k}}{\nu_1}\right)\right]\psi_{1,k}\end{aligned} \tag{23}$$

which yields a virtual controller $\alpha_{1,k}$ with the following form:

$$\alpha_{1,k} = \frac{1}{g_{1,k}}\left(-c_1 e_{1,k} + \dot{y}_d - \hat{\Theta}_{1,k}^{\mathrm{T}}\Phi_{1,k} - \hat{\varepsilon}_{1,k}\right) \tag{24}$$

where $\Phi_{1,k} \triangleq \Phi_1(X_{1,k})$, and $\hat{\Theta}_{1,k}$ and $\hat{\varepsilon}_{1,k}$ are the estimated values of Θ_1^* and $\bar{\varepsilon}_1$, respectively.

Substituting (24) into (23) yields

$$\begin{aligned}\dot{V}_{1,k} \leqslant\ & -c_1 z_{1,k}^2 + g_{1,k}z_{1,k}z_{2,k} - \tilde{\Theta}_{1,k}^{\mathrm{T}}\Phi_{1,k}z_{1,k} - z_{1,k}\tilde{\varepsilon}_{1,k} \\ & + \frac{1}{2}\left[1 - 2\tanh^2\left(\frac{z_{1,k}}{\nu_1}\right)\right]\psi_{1,k}\end{aligned} \tag{25}$$

where $\tilde{\Theta}_{1,k} = \hat{\Theta}_{1,k} - \Theta_1^*$ and $\tilde{\varepsilon}_{1,k} = \hat{\varepsilon}_{1,k} - \bar{\varepsilon}_1$.

Step i ($i = 2, \ldots, n-1$): From (1) and (7), the derivative of $e_{i,k}$ is calculated by

$$\begin{aligned}\dot{e}_{i,k} = & f_i\left(x_{i,k}\left(\varrho - \tau_i\right)\right) \\ & + g_{i,k}\left[\left(\beta_{i+1,k} - \alpha_{i,k}\right) + e_{i+1,k} + \alpha_{i,k}\right] \\ & + d_{i,k} - \dot{\beta}_{i,k}.\end{aligned} \tag{26}$$

Furthermore, in terms of (8)–(10) and (26), the derivative of $z_{i,k}$ is calculated as follows:

$$\begin{aligned}\dot{z}_{i,k} = & f_i\left(x_{i,k}\left(\varrho - \tau_i\right)\right) + g_{i,k}\left(\alpha_{i,k} + z_{i+1,k}\right) \\ & + c_i\gamma_{i,k} + c_i\delta_{i,k} + g_{i-1,k}\gamma_{i-1,k} + g_{i-1,k}\delta_{i-1,k} \\ & + d_{i,k} - \dot{\beta}_{i,k}.\end{aligned} \tag{27}$$

Select the candidate L–K functional as follows:

$$V_{i,k} = \frac{1}{2}z_{i,k}^2 + \frac{1}{2}\sum_{j=1}^{i}\int_{\varrho-\tau_j}^{\varrho}\rho_{i,j}^2\left(x_{j,k}\left(\tau\right)\right)d\tau. \tag{28}$$

Derivating of $V_{i,k}$ gives

$$\begin{aligned}\dot{V}_{i,k} = & z_{i,k}\left[g_{i,k}\left(z_{i+1,k}+\alpha_{i,k}\right) + c_i\gamma_{i,k} + c_i\delta_{i,k}\right. \\ & \left. + g_{i-1,k}\gamma_{i-1,k} + g_{i-1,k}\delta_{i-1,k} - \dot{\beta}_{i,k}\right] \\ & + z_{i,k}f_i\left(\bar{x}_{i,k}\left(\varrho - \tau_i\right)\right) + z_{i,k}d_{i,k} \\ & + \frac{1}{2}\sum_{j=1}^{i}\rho_{i,j}^2\left(x_{j,k}\right) - \frac{1}{2}\sum_{j=1}^{i}\rho_{i,j}^2\left(x_{j,k}\left(\varrho - \tau_j\right)\right).\end{aligned} \tag{29}$$

Similar to step 1, the right-hand side second and third terms of (29) are executed as follows:

$$z_{i,k}f_i\left(x_{i,k}\left(\varrho - \tau_i\right)\right) \leqslant \frac{i}{2}z_{i,k}^2\theta_i^2 + \frac{1}{2}\sum_{j=1}^{i}\rho_{i,j}^2\left(x_{j,k}\left(\varrho - \tau_j\right)\right) \tag{30}$$

and

$$z_{i,k}d_{i,k} \leqslant \frac{1}{2}z_{i,k}^2\mu_{i,k}^2 + \frac{1}{2}. \tag{31}$$

Taking (30) and (31) into (29) produces

$$\begin{aligned}\dot{V}_{i,k} \leqslant\ & z_{i,k}\left[g_{i,k}\left(z_{i+1,k}+\alpha_{i,k}\right) + c_i\gamma_{i,k} + c_i\delta_{i,k}\right. \\ & + g_{i-1,k}\gamma_{i-1,k} + g_{i-1,k}\delta_{i-1,k} - \dot{\beta}_{i,k} + \frac{i}{2}z_{i,k}\theta_i^2 \\ & \left. + \frac{1}{2}z_{i,k}\mu_{i,k}^2\right] + \frac{1}{2}\psi_{i,k}\end{aligned} \tag{32}$$

where $\psi_{i,k} = \sum_{j=1}^{i}\rho_{i,j}^2(x_{j,k}) + 1$.

Similar to (20), $(1/2)\psi_{i,k}$ is transformed into the following form:

$$\frac{1}{2}\psi_{i,k} = \tanh^2\left(\frac{z_{i,k}}{\nu_i}\right)\psi_{i,k} + \frac{1}{2}\left[1 - 2\tanh^2\left(\frac{z_{i,k}}{\nu_i}\right)\right]\psi_{i,k} \tag{33}$$

where ν_i is a positive constant.

Putting (33) into (32) provides

$$\begin{aligned}\dot{V}_{i,k} \leqslant\ & z_{i,k}\Bigg[g_{i,k}\left(z_{i+1,k}+\alpha_{i,k}\right) + c_i\gamma_{i,k} + c_i\delta_{i,k} \\ & + g_{i-1,k}\gamma_{i-1,k} + g_{i-1,k}\delta_{i-1,k} - \dot{\beta}_{i,k} \\ & + \underbrace{\frac{i}{2}z_{i,k}\theta_i^2 + \frac{1}{2}z_{i,k}\mu_{i,k}^2 + \frac{1}{z_{i,k}}\tanh^2\left(\frac{z_{i,k}}{\nu_i}\right)\psi_{i,k}}_{\eta_i}\Bigg] \\ & + \frac{1}{2}\left[1 - 2\tanh^2\left(\frac{z_{i,k}}{\nu_i}\right)\right]\psi_{i,k}.\end{aligned} \tag{34}$$

Using RBF NNs, η_i in (34) is approximated as follows:

$$\eta_i = \Theta_i^{*\mathrm{T}}\Phi_i\left(X_{i,k}\right) + \varepsilon_i\left(X_{i,k}\right) \tag{35}$$

where $X_{i,k} = [x_{1,k}, \ldots, x_{i,k}, \gamma_{1,k}, \ldots, \gamma_{i,k}, \delta_{1,k}, \ldots, \delta_{i,k}]^{\mathrm{T}}$.

Replacing the corresponding part of (34) with (35) yields the new form of (34) as follows:

$$\begin{aligned}\dot{V}_{i,k} \leqslant z_{i,k}\Big[&g_{i,k}\left(z_{i+1,k}+\alpha_{i,k}\right)+c_i\gamma_{i,k}+c_i\delta_{i,k}\\&+g_{i-1,k}\gamma_{i-1,k}+g_{i-1,k}\delta_{i-1,k}-\dot{\beta}_{i,k}\\&+\Theta_i^{*\mathrm{T}}\Phi_i\left(X_{i,k}\right)+\bar{\varepsilon}_i\left(X_{i,k}\right)\Big]\\&+\frac{1}{2}\left[1-2\tanh^2\left(\frac{z_{i,k}}{\nu_i}\right)\right]\psi_{i,k}\end{aligned}\tag{36}$$

which renders a virtual controller $\alpha_{i,k}$ presented by

$$\alpha_{i,k}=\frac{1}{g_{i,k}}\left(-c_ie_{i,k}-g_{i-1,k}e_{i-1,k}+\dot{\beta}_{i,k}-\hat{\Theta}_{i,k}^{\mathrm{T}}\Phi_{i,k}-\hat{\varepsilon}_{i,k}\right)\tag{37}$$

where $\Phi_{i,k} \triangleq \Phi_i(X_{i,k})$, and $\hat{\Theta}_{i,k}$ and $\hat{\varepsilon}_{i,k}$ are the estimated values of Θ_i^* and $\bar{\varepsilon}_i$, respectively.

Imposing the controller $\alpha_{i,k}$ on (36) supplies

$$\begin{aligned}\dot{V}_{i,k} \leqslant &-c_iz_{i,k}^2+g_{i,k}z_{i,k}z_{i+1,k}-g_{i-1,k}z_{i-1,k}z_{i,k}\\&-z_{i,k}\tilde{\Theta}_{i,k}^{\mathrm{T}}\Phi_{i,k}-z_{i,k}\tilde{\varepsilon}_{i,k}\\&+\frac{1}{2}\left[1-2\tanh^2\left(\frac{z_{i,k}}{\nu_i}\right)\right]\psi_{i,k}\end{aligned}\tag{38}$$

where $\tilde{\Theta}_{i,k}=\hat{\Theta}_{i,k}-\Theta_i^*$ and $\tilde{\varepsilon}_{i,k}=\hat{\varepsilon}_{i,k}-\bar{\varepsilon}_i$.

Step n: An actual controller is designed for the nth subsystem. Consistent with the preceding steps, the forms of $\dot{e}_{n,k}$ and $\dot{z}_{n,k}$ are first provided

$$\dot{e}_{n,k}=f_n\left(x_{n,k}\left(\varrho-\tau_n\right)\right)+g_{n,k}u\left(v_k\right)+d_{n,k}-\dot{\beta}_{n,k}\tag{39}$$

and

$$\begin{aligned}\dot{z}_{n,k}=&f_n\left(x_{n,k}\left(\varrho-\tau_n\right)\right)+g_{n,k}v_k+c_n\gamma_{n,k}\\&+c_n\delta_{n,k}+g_{n-1,k}\gamma_{n-1,k}+g_{n-1,k}\delta_{n-1,k}\\&+d_{n,k}-\dot{\beta}_{n,k}.\end{aligned}\tag{40}$$

Set the candidate L–K functional as follows:

$$V_{n,k}=\frac{1}{2}z_{n,k}^2+\frac{1}{2}\sum_{j=1}^{n}\int_{\varrho-\tau_j}^{\varrho}\rho_{n,j}^2\left(x_{j,k}\left(\tau\right)\right)d\tau.\tag{41}$$

Executing derivation operataion on $V_{n,k}$ produces

$$\begin{aligned}\dot{V}_{n,k}=&z_{n,k}\left[g_{n,k}v_k-\dot{\beta}_{n,k}+c_n\gamma_{n,k}+c_n\delta_{n,k}\right.\\&\left.+g_{n-1,k}\gamma_{n-1,k}+g_{n-1,k}\delta_{n-1,k}\right]\\&+z_{n,k}f_n\left(x_{n,k}\left(\varrho-\tau_n\right)\right)+z_{n,k}d_{n,k}\\&+\frac{1}{2}\sum_{j=1}^{n}\rho_{n,j}^2\left(x_{j,k}\right)-\frac{1}{2}\sum_{j=1}^{n}\rho_{n,j}^2\left(x_{j,k}\left(\varrho-\tau_j\right)\right).\end{aligned}\tag{42}$$

The right-hand side second and third terms of (42) are treated by

$$z_{n,k}f_n\left(x_{n,k}\left(\varrho-\tau_n\right)\right)\leqslant\frac{n}{2}z_{n,k}^2\theta_n^2+\frac{1}{2}\sum_{j=1}^{n}\rho_{n,j}^2\left(x_{j,k}\left(\varrho-\tau_j\right)\right)\tag{43}$$

and

$$z_{n,k}d_{n,k}\leqslant\frac{1}{2}z_{n,k}^2\mu_{n,k}^2+\frac{1}{2}.\tag{44}$$

From (43) and (44), (42) is further expressed as follows:

$$\begin{aligned}\dot{V}_{n,k}\leqslant z_{n,k}&\left[g_{n,k}v_k+c_n\gamma_{n,k}+c_n\delta_{n,k}+g_{n-1,k}\gamma_{n-1,k}\right.\\&\left.+g_{n-1,k}\delta_{n-1,k}-\dot{\beta}_{n,k}+\frac{n}{2}z_{n,k}\theta_n^2+\frac{1}{2}z_{n,k}\mu_n^2\right]\\&+\frac{1}{2}\psi_{n,k}\end{aligned}\tag{45}$$

where $\psi_{n,k}=\sum_{j=1}^{n}\rho_{n,j}^2(x_{j,k})+1$.

Similar to (33), $(1/2)\psi_{n,k}$ is transformed into the following form:

$$\frac{1}{2}\psi_{n,k}=\tanh^2\left(\frac{z_{n,k}}{\nu_n}\right)\psi_{n,k}+\frac{1}{2}\left[1-2\tanh^2\left(\frac{z_{n,k}}{\nu_n}\right)\right]\psi_{n,k}\tag{46}$$

where ν_n is a positive constant.

Taking (46) into (45) gives

$$\begin{aligned}\dot{V}_{n,k}\leqslant z_{n,k}&\left[g_{n,k}v_k+c_n\gamma_{n,k}+c_n\delta_{n,k}+g_{n-1,k}\gamma_{n-1,k}\right.\\&+g_{n-1,k}\delta_{n-1,k}-\dot{\beta}_{n,k}\\&\left.\underbrace{+\frac{n}{2}z_{n,k}\theta_n^2+\frac{1}{2}z_{n,k}\mu_{n,k}^2+\frac{1}{z_{n,k}}\tanh^2\left(\frac{z_{n,k}}{\nu_n}\right)\psi_{n,k}}_{\eta_n}\right]\\&+\frac{1}{2}\left[1-2\tanh^2\left(\frac{z_{n,k}}{\nu_n}\right)\right]\psi_{n,k}.\end{aligned}\tag{47}$$

Resorting to RBF NNs, η_n in (47) is approximated as follows:

$$\eta_n=\Theta_n^{*\mathrm{T}}\Phi_n\left(X_{n,k}\right)+\varepsilon_n\left(X_{n,k}\right)\tag{48}$$

where $X_{n,k}=[x_{1,k},\ldots,x_{n,k},\gamma_{1,k},\ldots,\gamma_{n,k},\delta_{1,k},\ldots,\delta_{n,k}]^{\mathrm{T}}$.

Taking (48) into (47) supplies

$$\begin{aligned}\dot{V}_{n,k}\leqslant&z_{n,k}\left[g_{n,k}v_k+c_n\gamma_{n,k}+c_n\delta_{n,k}+g_{n-1,k}\gamma_{n-1,k}+g_{n-1,k}\right.\\&\left.\times\delta_{i-1,k}-\dot{\beta}_{n,k}+\Theta_n^{*\mathrm{T}}\Phi_n\left(X_{n,k}\right)+\bar{\varepsilon}_n\left(X_{n,k}\right)\right]\\&+\frac{1}{2}\left[1-2\tanh^2\left(\frac{z_{n,k}}{\nu_n}\right)\right]\psi_{n,k}.\end{aligned}\tag{49}$$

The actual controller is constructed as follows:

$$v_k=\frac{1}{g_{n,k}}\left(-c_ne_{n,k}-g_{n-1,k}e_{n-1,k}+\dot{\beta}_{n,k}-\hat{\Theta}_{n,k}^{\mathrm{T}}\Phi_{n,k}-\hat{\varepsilon}_{n,k}\right)\tag{50}$$

where $\Phi_{n,k} \triangleq \Phi_n(X_{n,k})$, and $\hat{\Theta}_{n,k}$ and $\hat{\varepsilon}_{n,k}$ are the estimated values of Θ_n^* and $\bar{\varepsilon}_n$, respectively.

Combining (50) and (49) yields

$$\begin{aligned}\dot{V}_{n,k}\leqslant&-c_nz_{n,k}^2-g_{n-1,k}z_{n-1,k}z_{n,k}-z_{n,k}\tilde{\Theta}_{n,k}^{\mathrm{T}}\Phi_{n,k}\\&-z_{n,k}\tilde{\varepsilon}_{n,k}+\frac{1}{2}\left[1-2\tanh^2\left(\frac{z_{n,k}}{\nu_n}\right)\right]\psi_{n,k}\end{aligned}\tag{51}$$

where $\tilde{\Theta}_{n,k} = \hat{\Theta}_{n,k} - \Theta_n^*$ and $\tilde{\varepsilon}_{n,k} = \hat{\varepsilon}_{n,k} - \bar{\varepsilon}_n$. Moreover, the updating laws are given by

$$\begin{cases} \hat{\Theta}_{i,k} = \text{proj}\left(\hat{\Theta}_{i,k}^{\nabla}\right) \\ \hat{\Theta}_{i,k}^{\nabla} = \hat{\Theta}_{i,k-1} + \Gamma_i z_{i,k} \Phi_{i,k} \\ \hat{\Theta}_{i,0} = 0, \quad \varrho \in [0, T] \end{cases} \tag{52}$$

and

$$\begin{cases} (1 - q_i)\, \dot{\hat{\varepsilon}}_{i,k} = -q_i \hat{\varepsilon}_{i,k} + q_i \hat{\varepsilon}_{i,k-1} + K_i z_{i,k} \\ \hat{\varepsilon}_{i,k}(0) = \hat{\varepsilon}_{i,k-1}(T) \\ \hat{\varepsilon}_{i,0} = 0, \quad \varrho \in [0, T] \end{cases} \tag{53}$$

where $\Gamma_i > 0$, $K_i > 0$, and $0 < q_i < 1$ are learning gains. Assume that each element of $\text{proj}(\hat{\Theta}_{i,k}^{\nabla})$ has the same upper and lower bounds. This assumption is commonly encountered and often subjected to parameter restrictions in practical applications, driven by considerations of safety and performance [46]. To be more intuitive, this assumption is expressed in the following form:

$$\text{proj}\left(\hat{\Theta}_{j,i,k}^{\nabla}\right) = \begin{cases} \Theta_{j,i}^{\min}, & \hat{\Theta}_{j,i,k}^{\nabla} < \Theta_{j,i}^{\min} \\ \hat{\Theta}_{j,i,k}^{\nabla}, & \Theta_{j,i}^{\min} \le \hat{\Theta}_{j,i,k}^{\nabla} \le \Theta_{j,i}^{\max} \\ \Theta_{j,i}^{\max}, & \hat{\Theta}_{j,i,k}^{\nabla} > \Theta_{j,i}^{\max} \end{cases} \tag{54}$$

where $\hat{\Theta}_{j,i,k}^{\nabla}$ denotes the jth element of $\hat{\Theta}_{i,k}^{\nabla}$, and $\Theta_{j,i}^{\min}$ and $\Theta_{j,i}^{\max}$ are the minimum and maximum estimated values of $\hat{\Theta}_{j,i,k}^{\nabla}$.

Remark 3: The backstepping method is adopted to deal with the unimplemented part of the command filter and input saturation via (8) and (9). However, this method is determined by the design of the auxiliary systems with known $g_{i,k}$.

Remark 4: A differential updating law (53) is employed to estimate the upper bound of neural networks error $\bar{\varepsilon}_i$, aiming to further improve the estimation accuracy of RBF NNs. Compared with [37], the utilization of (53) can effectively reduce the upper bounds of tracking error and compensation error. However, it necessitates the utilization of first-order derivatives of the parameters and the adjustment of an additional gain q_i.

Before demonstrating error convergence, the following lemmas are provided concerning the simplification of the projection term $\text{proj}(\hat{\Theta}_{i,k}^{\nabla})$ and the boundedness of the auxiliary system states.

Lemma 4 [29]: For any small positive constant ϵ and time T_0, there exists a sufficiently large bandwidth ω_i, such that $\beta_{i,k} - \alpha_{i-1,k}$ exponentially converges to ϵ neighborhood of the origin for $\varrho \in [0, T_0]$, $|\beta_{i,k} - \alpha_{i-1,k}| \le \epsilon$ for $\varrho \in [T_0, T]$.

Lemma 5 [20]: The states of auxiliary system (8) are bounded by

$$\|\gamma_k\| \le \frac{\epsilon g_{\max}}{2c_0} \tag{55}$$

where $\gamma_k = [\gamma_{1,k}, \ldots, \gamma_{n,k}]^{\mathrm{T}}$ and $c_0 = (1/2)\min(c_i)$.

Lemma 6: The states of auxiliary system (9) are bounded by

$$\|\delta_k\| \le \sqrt{\frac{\Delta u_{\max} g_{\max}}{2c_0}} \tag{56}$$

where $\delta_k = [\delta_{1,k}, \ldots, \delta_{2,k}]^{\mathrm{T}}$ and $c_0 = (1/2)\min(c_i)$. $\Delta u_{\max}$ is the upper bound for Δu_k if Δu_k is bounded.

Proof: Inspired by [20], define the Lyapunov function $V_\delta = (1/2)\|\delta_k\|^2$. From (9), the derivative of V_δ is shown as follows:

$$\begin{aligned} \dot{V}_\delta &= -\sum_{i=1}^{n} c_i \delta_{i,k}^2 + g_{n,k} \Delta u_k \\ &\le -2c_0 \|\delta_k\|^2 + g_{\max} \Delta u_{\max} \\ &\le -4c_0 V_\delta + g_{\max} \Delta u_{\max}. \end{aligned} \tag{57}$$

Multiplying (57) by $e^{4c_0\varrho}$ leads to

$$\dot{V}_\delta e^{4c_0\varrho} \le -4c_0 e^{4c_0\varrho} V_\delta + g_{\max} \Delta u_{\max} e^{4c_0\varrho} \tag{58}$$

which gives

$$V_\delta \le V_\delta(0)\, e^{-4c_0\varrho} + \frac{g_{\max} \Delta u_{\max}}{4c_0}. \tag{59}$$

It is deduced from (59) that

$$\|\delta_k\| \le \sqrt{\frac{g_{\max} \Delta u_{\max}}{2c_0}}. \tag{60}$$

□

After presenting the controller and updating laws, Theorem 1 provides the relevant proof of error convergence.

Theorem 1: Define the set $\Omega_{z_i} = \{z_{i,k} || z_{i,k}| < 0.8814 v_i\}$. For strict-feedback system (1) under Assumptions 1–6, the bounded convergence of tracking error $e_{i,k}$ and compensation error $z_{i,k}$ are guaranteed by virtual controller (24), (37), actual controller (50), and updating laws (52), (53) for $\varrho \in [0, T]$ as the iteration number k goes to infinity, i.e., $\lim_{k\to\infty} |z_{i,k}| \in \Omega_{z_i}$ and $|e_{i,k}| \le 0.8814 v_i + (\epsilon g_{\max})/(2c_0) + ((\Delta u_{\max} g_{\max})/(2c_0))^{1/2}$.

Proof: A CEF at the kth iteration is chosen as follows:

$$\begin{cases} E_k(\varrho) = E_{1,k}(\varrho) + E_{2,k}(t) + E_{3,k}(\varrho) \\ E_{1,k}(\varrho) = \sum_{i=1}^{n} V_{i,k} \\ E_{2,k}(\varrho) = \sum_{i=1}^{n} \int_0^{\varrho} \frac{1}{2\Gamma_i} \tilde{\Theta}_{i,k}^{\mathrm{T}} \Theta_{i,k} d\tau \\ E_{3,k}(\varrho) = \sum_{i=1}^{n} \frac{q_i}{2K_i} \int_0^{\varrho} \tilde{\varepsilon}_{i,k}^2 d\tau + \sum_{i=1}^{n} \frac{1 - q_i}{2K_i} \tilde{\varepsilon}_{i,k}^2. \end{cases} \tag{61}$$

On the one hand, taking into account the scenario $z_{i,k} \notin \Omega_{z_i}$, by Lemma 3, it is inferred that $\dot{E}_{1,k}$ can be derived in the following form:

$$\dot{E}_{1,k} \le -\sum_{i=1}^{n} c_i z_{i,k}^2 - \sum_{i=1}^{n} z_{i,k} \tilde{\Theta}_{i,k}^{\mathrm{T}} \Phi_{i,k} - \sum_{i=1}^{n} z_{i,k} \tilde{\varepsilon}_{i,k}. \tag{62}$$

Step A (Difference of $\boldsymbol{E_k(\varrho)}$): Consider the difference of $E_k(T)$ at the kth iteration

$$\Delta E_k(T) = \Delta E_{1,k}(T) + \Delta E_{2,k}(T) + \Delta E_{3,k}(T). \tag{63}$$

Initially, the derivation of $\Delta E_{1,k}(T)$ is executed as follows:

$$\Delta E_{1,k}(T) = \int_0^{\mathrm{T}} \dot{E}_{1,k}(\tau)\, d\tau + E_{1,k}(0) - E_{1,k-1}(0)$$

$$-\left(E_{1,k-1}(T)-E_{1,k-1}(0)\right). \quad (64)$$

According to Assumptions 1 and 2, setting $\gamma_{i,k}(0) = \delta_{i,k}(0) = 0$, one has

$$E_{1,k}(0) = E_{1,k-1}(0) = \sum_{i=1}^{n}\sum_{j=1}^{i}\int_{-\tau_j}^{0}\rho_{i,j}^2\left(\Upsilon_i(\tau)\right)d\tau \quad (65)$$

and

$$E_{1,k-1}(T) - E_{1,k-1}(0) = E_{1,k-1}(T) \geqslant 0. \quad (66)$$

Substituting (65) and (66) into (64) yields

$$\Delta E_{1,k}(T) \leqslant -\sum_{i=1}^{n}\int_0^{\mathrm{T}} c_i z_{i,k}^2 d\tau - \sum_{i=1}^{n}\int_0^{\mathrm{T}} z_{i,k}\tilde{\Theta}_{i,k}^{\mathrm{T}}\Phi_{i,k}d\tau - \sum_{i=1}^{n}\int_0^{\mathrm{T}} z_{i,k}\tilde{\varepsilon}_{i,k}d\tau. \quad (67)$$

From Lemma 2, the derivation of $\Delta E_{2,k}(T)$ is

$$\begin{aligned}
&\Delta E_{2,k}(T)\\
&= -\sum_{i=1}^{n}\frac{1}{2\Gamma_i}\int_0^{\mathrm{T}}\left(\hat{\Theta}_{i,k}-\hat{\Theta}_{i,k-1}\right)^{\mathrm{T}}\left(\hat{\Theta}_{i,k}-\hat{\Theta}_{i,k-1}\right)d\tau\\
&\quad+\sum_{i=1}^{n}\frac{1}{\Gamma_i}\int_0^{\mathrm{T}}\left(\hat{\Theta}_{i,k}^{\nabla}-\mathrm{proj}\left(\hat{\Theta}_{i,k}^{\nabla}\right)\right)^{\mathrm{T}}\left(\Theta_i^{*}-\mathrm{proj}\left(\hat{\Theta}_{i,k}^{\nabla}\right)\right)d\tau\\
&\quad+\sum_{i=1}^{n}\frac{1}{\Gamma_i}\int_0^{\mathrm{T}}\left(\hat{\Theta}_{i,k}^{\nabla}-\hat{\Theta}_{i,k-1}\right)^{\mathrm{T}}\tilde{\Theta}_{i,k}d\tau\\
&\leqslant\sum_{i=1}^{n}\int_0^{\mathrm{T}} z_{i,k}\tilde{\Theta}_{i,k}\Phi_{i,k}d\tau. \quad (68)
\end{aligned}$$

Calculating $\Delta E_{3,k}(T)$ in (63) gives

$$\begin{aligned}
&\Delta E_{3,k}(T)\\
&=\sum_{i=1}^{n}\int_0^{\mathrm{T}}\frac{q_i}{2K_i}\left(\tilde{\varepsilon}_{i,k}^2-\tilde{\varepsilon}_{i,k-1}^2\right)d\tau\\
&\quad+\sum_{i=1}^{n}\frac{1-q_i}{2\Gamma_i}\left[\tilde{\varepsilon}_{i,k}^2(0)-\tilde{\varepsilon}_{i,k-1}^2(T)\right]\\
&\quad+\sum_{i=1}^{n}\int_0^{\mathrm{T}} z_{i,k}\tilde{\varepsilon}_{i,k}d\tau-\sum_{i=1}^{n}\int_0^{\mathrm{T}}\frac{q_i}{K_i}\tilde{\varepsilon}_{i,k}\left(\hat{\varepsilon}_{i,k}-\hat{\varepsilon}_{i,k-1}\right)d\tau.
\end{aligned} \quad (69)$$

Resorting to $\hat{\varepsilon}_{i,k}-\hat{\varepsilon}_{i,k-1} = \tilde{\varepsilon}_{i,k}-\tilde{\varepsilon}_{i,k-1}$, one has

$$\begin{aligned}
&\Delta E_{3,k}(T)\\
&=\sum_{i=1}^{n}\frac{1-q_i}{2\Gamma_i}\left[\tilde{\varepsilon}_{i,k}^2(0)-\tilde{\varepsilon}_{i,k-1}^2(T)\right]+\sum_{i=1}^{n}\int_0^{\mathrm{T}} z_{i,k}\tilde{\varepsilon}_{i,k}d\tau\\
&\quad-\sum_{i=1}^{n}\int_0^{\mathrm{T}}\frac{q_i}{2K_i}\left(\tilde{\varepsilon}_{i,k}-\tilde{\varepsilon}_{i,k-1}\right)^2 d\tau\\
&\leqslant\sum_{i=1}^{n}\int_0^{\mathrm{T}} z_{i,k}\tilde{\varepsilon}_{i,k}d\tau.
\end{aligned} \quad (70)$$

Then, substituting (67), (68), and (70) into (63) leads to

$$\Delta E_k(T) \leq -\sum_{i=1}^{n}\int_0^{\mathrm{T}} c_i z_{i,k}^2 d\tau. \quad (71)$$

Step B (Boundedness of $\boldsymbol{E_1(\varrho)}$): From $\Delta E_k(\varrho)$, the boundedness of $E_k(T)$ can be guaranteed by $E_1(T)$. Thus, a boundedness proof for $E_1(\varrho)$ is given as follows:

$$\dot{E}_1(\varrho) = \dot{E}_{1,1}(\varrho) + \dot{E}_{2,1}(\varrho) + \dot{E}_{3,1}(\varrho). \quad (72)$$

The first term $\dot{E}_{1,1}(\varrho)$ of (72) is calculated as follows:

$$\dot{E}_{1,1}(\varrho) = -\sum_{i=1}^{n}\left(c_i z_{i,1}^2 + z_{i,1}\tilde{\Theta}_{i,1}^{\mathrm{T}}\Phi_{i,1} + z_{i,1}\tilde{\varepsilon}_{i,1}\right). \quad (73)$$

Subsequently, dealing with the second term $\dot{E}_{2,1}(\varrho)$ of (72) produces

$$\dot{E}_{2,1}(\varrho) = \sum_{i=1}^{n}\frac{1}{2\Gamma_i}\left(\tilde{\Theta}_{i,1}^{\mathrm{T}}\tilde{\Theta}_{i,1} - \tilde{\Theta}_{i,0}^{\mathrm{T}}\tilde{\Theta}_{i,0}\right) + \sum_{i=1}^{n}\frac{1}{2\Gamma_i}\tilde{\Theta}_{i,0}^{\mathrm{T}}\tilde{\Theta}_{i,0}. \quad (74)$$

According to the updating law (52), (74) is transformed into

$$\dot{E}_{2,1}(\varrho) \leqslant \sum_{i=1}^{n} z_{i,1}\tilde{\Theta}_{i,1}^{\mathrm{T}}\Phi_{i,1} + \sum_{i=1}^{n}\frac{1}{2\Gamma_i}\Theta_i^{*\mathrm{T}}\Theta_i^{*}. \quad (75)$$

Finally, operating the third term in (72) yields

$$\begin{aligned}
\dot{E}_{3,1}(\varrho) &\leqslant \sum_{i=1}^{n}\frac{q_i}{2K_i}\left(\hat{\varepsilon}_{i,1}-\tilde{\varepsilon}_{i,1}\right)^2 + \sum_{i=1}^{n} z_{i,1}\tilde{\varepsilon}_{i,1}\\
&\leqslant \sum_{i=1}^{n}\frac{q_i}{2K_i}\tilde{\varepsilon}_i^2 + \sum_{i=1}^{n} z_{i,1}\tilde{\varepsilon}_{i,1}.
\end{aligned} \quad (76)$$

Taking (73)–(76) into (72) gives

$$\dot{E}_1(\varrho) \leq \sum_{i=1}^{n}\frac{1}{2\Gamma_i}\Theta_i^{*\mathrm{T}}\Theta_i^{*} + \sum_{i=1}^{n}\frac{q_i}{2K_i}\tilde{\varepsilon}_i^2 \quad (77)$$

which indicates the boundedness of $E_1(t)$.

Step C (Convergence Property): Based on (71) and (77), one has

$$\begin{aligned}
\lim_{k\to\infty} E_k(T) &= E_1(T) + \lim_{k\to\infty}\sum_{j=2}^{k}\sum_{i=1}^{n} E_n(T)\\
&\leq E_1(T) - \lim_{k\to\infty}\sum_{j=2}^{k}\sum_{i=1}^{n}\int_0^{\mathrm{T}} c_i z_{i,j}^2 d\tau.
\end{aligned} \quad (78)$$

Considering the positiveness of $E_k(T)$ and the boundedness of $E_1(\varrho)$, (78) indicates that

$$\lim_{k\to\infty}\int_0^{\mathrm{T}} z_{i,k}^2 d\tau = 0. \quad (79)$$

Therefore, $\lim_{k\to\infty}|z_{i,k}| \in \Omega_{z_i}$ is satisfied. Since the boundedness of E_k has been proved, the components $z_{i,k}$, $\tilde{\Theta}_{i,k}$, and $\tilde{\varepsilon}_{i,k}$ of E_k are bounded, so does the boundedness of $e_{i,k}$, $\hat{\Theta}_{i,k}$, and $\hat{\varepsilon}_{i,k}$. Thus, the virtual controller $\alpha_{i,k}$ and the actual controller v_k

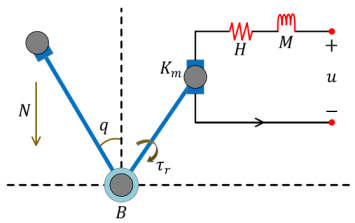

Fig. 1. Single-link manipulator.

are bounded. Moreover, Δu_k is bounded and satisfies $\Delta u_k \leqslant \Delta u_{\max}$, where $\Delta u_{\max}$ is a finite constant.

If $z_{i,k} \in \Omega_{z_i}$, from (8)–(10), it is obtained that

$$|e_{i,k}| \leqslant |z_{i,k}| + \|\gamma_k\| + \|\delta_k\|. \tag{80}$$

Based on Lemmas 5 and 6, one has

$$|e_{i,k}| \leqslant 0.8814\nu_i + \frac{\epsilon g_{\max}}{2c_0} + \sqrt{\frac{\Delta u_{\max} g_{\max}}{2c_0}}. \tag{81}$$

This completes the proof. □

Remark 5: Without updating law (53), (71) transforms into $\Delta E_k(T) \leq -\sum_{i=1}^{n}\int_0^{\mathrm{T}} c_i z_{i,k}^2 d\tau + \sum_{i=1}^{n}\bar{\varepsilon}_i$, which changes into $\lim_{k\to\infty}\int_0^{\mathrm{T}} z_{i,k}^2 d\tau \leqslant \sum_{i=1}^{n}\bar{\varepsilon}_i$. In this scenario, the convergence proof of the compensated error is similar to [37].

IV. Illustrative Example

Consider a single-link manipulator [47] in Fig. 1.

It is presented by

$$\begin{cases} D\ddot{q} + B\dot{q} + N\sin(q) = \tau_r + \tau_d \\ M\dot{\tau}_r + H\tau_r = u - K_m\dot{q} \end{cases} \tag{82}$$

where $D = 1.0\ \mathrm{kg\cdot m^2}$, $B = 1.0\ \mathrm{Nm\cdot s/rad}$, $N = 10\ \mathrm{m/s^2}$, and $\tau_d = \sin(q(\varrho - d))$ with $d = 0.4$ s, $M = 1.0$ H, $H = 0.5\ \Omega$, and $K_m = 10$ Nm/A.

In order to employ the backstepping method, (82) is reconstructed based on q, $\dot{q}$, and τ_r

$$\begin{cases} \dot{x}_{1,k} = x_{2,k} \\ \dot{x}_{2,k} = x_{3,k} - Bx_{2,k} + \sin\left(x_{1,k}(\varrho - d)\right) - N\sin\left(x_{1,k}\right) \\ \dot{x}_{3,k} = u_k - K_m x_{2,k} - Hx_{3,k} \end{cases} \tag{83}$$

where $x_{1,k} = q$, $x_{2,k} = \dot{q}$, and $x_{3,k} = \tau_r$.

To compensate the unimplemented part of the command filter and input saturation, (8) and (9) are

$$\begin{cases} \dot{\gamma}_{1,k} = -c_1\gamma_{1,k} + \left(\beta_{2,k} - \alpha_{1,k}\right) + \gamma_{2,k} \\ \dot{\gamma}_{2,k} = -c_2\gamma_{2,k} + \left(\beta_{3,k} - \alpha_{2,k}\right) + \gamma_{3,k} - \gamma_{1,k} \\ \dot{\gamma}_{3,k} = -c_3\gamma_{3,k} - \gamma_{2,k} \end{cases}$$

and

$$\begin{cases} \dot{\delta}_{1,k} = -c_1\delta_{1,k} + \delta_{2,k} \\ \dot{\delta}_{2,k} = -c_2\delta_{2,k} + \delta_{3,k} - \delta_{1,k} \\ \dot{\delta}_{3,k} = -c_3\delta_{3,k} + \Delta u_k - \delta_{2,k}. \end{cases}$$

The coordinate transformations and compensation error of (83) are $e_{1,k} = y_{1,k} - y_d$, $e_{i,k} = x_{i,k} - \beta_{i,k}$, and $z_{i,k} = e_{i,k} - \gamma_{i,k} - \delta_{i,k}$, where $y_{1,k} = x_{1,k}$ is the output of system (83).

Based on the controller design process, one has $z_{2,k}\sin(x_{1,k}) \leqslant (1/2)z_{2,k}^2 + (1/2)\sin^2(x_{1,k})$ and $z_{3,k}(-K_m x_{2,k} - Hx_{3,k}) \leqslant (1/2)z_{3,k}^2 + (1/2)(K_m x_{2,k} + Hx_{3,k})^2$.

Utilize RBF NNs to estimate unknown terms as follows:

$$\Theta_2^{*\mathrm{T}}\Phi_{2,k} + \varepsilon_2 = \frac{1}{z_{2,k}}\tanh^2\left(\frac{z_{2,k}}{\nu_2}\right)\sin^2\left(x_{1,k}\right) - N\sin\left(x_{1,k}\right) - Bx_{2,k}$$

and

$$\Theta_3^{*\mathrm{T}}\Phi_{3,k} + \varepsilon_3 = \frac{1}{z_{3,k}}\tanh^2\left(\frac{z_{3,k}}{\nu_3}\right)\left(K_m x_{2,k} + Hx_{3,k}\right).$$

Furthermore, the controllers and updating laws are constructed as follows:

$$\alpha_{1,k} = -c_1 e_{1,k} + \dot{x}_d \tag{84}$$

$$\alpha_{2,k} = -c_2 e_{2,k} - e_{1,k} + \dot{\beta}_{2,k} - \frac{1}{2}z_{2,k} - \hat{\Theta}_{2,k}^{\mathrm{T}}\Phi_{2,k} - \hat{\varepsilon}_{2,k} \tag{85}$$

$$u_k = -c_3 e_{3,k} - e_{2,k} + \dot{\beta}_{3,k} - \frac{1}{2}z_{3,k} - \hat{\Theta}_{3,k}^{\mathrm{T}}\Phi_{3,k} - \hat{\varepsilon}_{3,k} \tag{86}$$

$$\begin{cases} \hat{\Theta}_{2,k} = \mathrm{proj}\left(\hat{\Theta}_{2,k}^{\nabla}\right) \\ \hat{\Theta}_{2,k}^{\nabla} = \hat{\Theta}_{2,k-1} + \Gamma_2 z_{2,k}\Phi_{2,k} \\ \hat{\Theta}_{2,0} = 0, \quad \varrho \in [0, T] \end{cases} \tag{87}$$

$$\begin{cases} \hat{\Theta}_{3,k} = \mathrm{proj}\left(\hat{\Theta}_{3,k}^{\nabla}\right) \\ \hat{\Theta}_{3,k}^{\nabla} = \hat{\Theta}_{3,k-1} + \Gamma_3 z_{3,k}\Phi_{3,k} \\ \hat{\Theta}_{3,0} = 0, \quad \varrho \in [0, T] \end{cases} \tag{88}$$

$$\begin{cases} (1 - q_2)\,\dot{\hat{\varepsilon}}_{2,k} = -q_2\hat{\varepsilon}_{2,k} + q_2\hat{\varepsilon}_{2,k-1} + K_2 z_{2,k} \\ \hat{\varepsilon}_{2,k}(0) = \hat{\varepsilon}_{2,k-1}(T) \\ \hat{\varepsilon}_{2,0} = 0, \quad \varrho \in [0, T] \end{cases} \tag{89}$$

$$\begin{cases} (1 - q_3)\,\dot{\hat{\varepsilon}}_{3,k} = -q_3\hat{\varepsilon}_{3,k} + q_3\hat{\varepsilon}_{3,k-1} + K_3 z_{3,k} \\ \hat{\varepsilon}_{3,k}(0) = \hat{\varepsilon}_{3,k-1}(T) \\ \hat{\varepsilon}_{3,0} = 0, \quad \varrho \in [0, T] \end{cases} \tag{90}$$

where $c_1 = c_2 = c_3 = 0.5$, $\kappa_2 = \kappa_3 = 50$, $\Gamma_2 = \Gamma_3 = 0.1$, $q_2 = q_3 = 0.6$, $K_2 = K_3 = 0.1$, $u_m = 5$, the iteration number $k = 80$, and the runtime for each iteration $T = 10$ s. Set $X_{2,k} = [x_{1,k}; x_{2,k}; \gamma_{1,k}; \gamma_{2,k}; \delta_{1,k}; \delta_{2,k}]$, $X_{3,k} = [x_{1,k}; x_{2,k}; x_{3,k}; \gamma_{1,k}; \gamma_{2,k}; \gamma_{3,k}; \delta_{1,k}; \delta_{2,k}; \delta_{3,k}]$, $a_2 = 1/\varsigma(2\iota - \varsigma)[1; 1.5; -1; -1]$ with $\varsigma = 10$ and $\iota = 1, \ldots, \varsigma$, $a_3 = 1/\varsigma(2\iota - \varsigma)[1; 1.5; -1; -1; -1; -1]$ with $\varsigma = 10$ and $\iota = 1, \ldots, \varsigma$, $\sigma_2 = \sigma_3 = 5$, $y_d = -0.1(\cos(\varrho) - 1)$, $x_{1,k}(0) = x_{2,k}(0) = x_{3,k}(0) = 0$, $\gamma_{1,k}(0) = \gamma_{2,k}(0) = \gamma_{3,k}(0) = 0$, and $\delta_{1,k}(0) = \delta_{2,k}(0) = \delta_{3,k}(0) = 0$.

Applying Theorem 1 and the method in [29], defining $|e_{1,k}|_{\max} \triangleq \sup_{t\in[0,T]}|e_{1,k}|$ and $\|z_{i,k}\|_{\max} \triangleq \sup_{t\in[0,T]}\|z_{i,k}\|$ yields Figs. 2 and 3 to exhibit the input without saturation and with saturation under different iterations, respectively. Fig. 4 demonstrates the maximum compensation error with input saturation along the iteration axis. Without considering input saturation, Figs. 5 and 6 show the comparative evolution of the maximum compensation error and maximum tracking

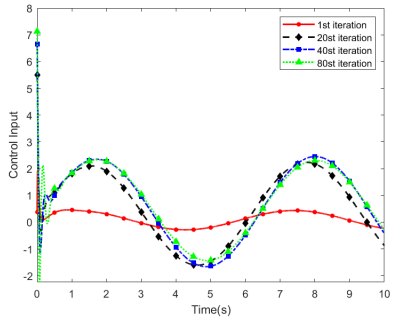

Fig. 2. Input without saturation.

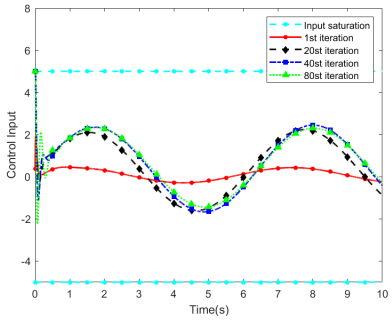

Fig. 3. Input with saturation.

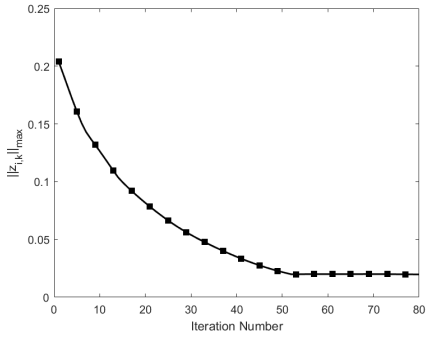

Fig. 4. $\|z_{i,k}\|_{\max}$ with input saturation.

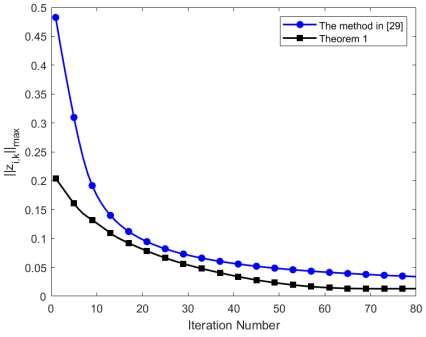

Fig. 5. Comparison of $\|z_{i,k}\|_{\max}$.

error along the iteration axis, respectively. Moreover, Fig. 7 is provided to address the tracking performance under different iteration numbers.

Seeing from Figs. 5 and 6, the maximum tracking error and maximum compensation error are smaller than these provided in [29]. Moreover, all errors converge along the iteration axis, demonstrating the feasibility of algorithm (84)–(90). According to Fig. 7, the iteration performance is almost the same to the tracking trajectory when the iteration number

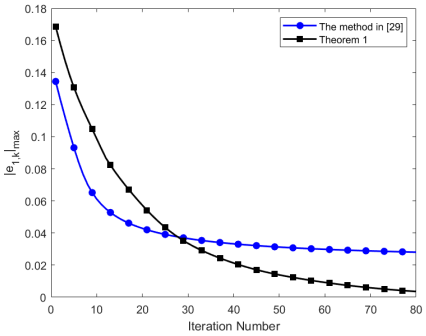

Fig. 6. Comparison of $|e_{1,k}|_{\max}$.

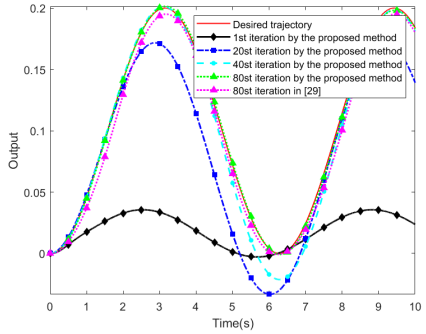

Fig. 7. Comparison of tracking performance under different iterations.

is large enough. In addition, this figure also shows a better tracking performance than that of [29] at the 80th iteration. In summary, all the simulation curves show that the proposed method is better than that in [29].

V. Conclusion

To address the control of strict-feedback systems with input saturation and unknown state delays, a command filter is adopted to circumvent the continuous differentiation of the virtual controller first. Then, auxiliary systems are designed to offset the unimplemented portion of the command filter and input saturation. Third, unknown state delays are treated by the constructed L–K functionals, and RBF NNs are employed to estimate the induced unknown terms. Fourth, a CEF is devised to ensure the convergence of tracking and compensatory errors. At last, a simulation study validates the superiority of the exploited algorithm over the existing result. The future work will focus on high order systems with initial errors.

References

[1] D. A. Bristow, M. Tharayil, and A. G. Alleyne, "A survey of iterative learning control," *IEEE Control Syst. Mag.*, vol. 26, no. 3, pp. 96–114, Jun. 2006.

[2] T. Meng and W. He, "Iterative learning control of a robotic arm experiment platform with input constraint," *IEEE Trans. Ind. Electron.*, vol. 65, no. 1, pp. 664–672, Jan. 2018.

[3] D. Huang, W. Yang, T. Huang, N. Qin, Y. Chen, and Y. Tan, "Iterative learning operation control of high-speed trains with adhesion dynamics," *IEEE Trans. Control Syst. Technol.*, vol. 29, no. 6, pp. 2598–2608, Nov. 2021.

[4] S. Su, Q. Zhu, J. Liu, T. Tang, Q. Wei, and Y. Cao, "A data-driven iterative learning approach for optimizing the train control strategy," *IEEE Trans. Ind. Informat.*, vol. 19, no. 7, pp. 7885–7893, Jul. 2023.

[5] J. Dong and B. He, "Novel fuzzy PID-type iterative learning control for quadrotor UAV," *Sensors*, vol. 19, no. 1, p. 24, Dec. 2018.

[6] P. Borchers, M. Walter, S. Leonhardt, D. Telyshev, and A. Pugovkin, "Flow profile generation for a left ventricular assist device using iterative learning control," *Current Directions Biomed. Eng.*, vol. 7, no. 2, pp. 279–282, Oct. 2021.

[7] R. Chi, Y. Lv, and B. Huang, "Distributed iterative learning temperature control for multi-zone HVAC system," *J. Franklin Inst.*, vol. 357, no. 2, pp. 810–831, Jan. 2020.

[8] X. Yu and T. Chen, "Distributed iterative learning control of nonlinear multiagent systems using controller-based dynamic linearization method," *IEEE Trans. Cybern.*, vol. 54, no. 8, pp. 4489–4501, Aug. 2024.

[9] D. Meng and J. Zhang, "Convergence analysis of robust iterative learning control against nonrepetitive uncertainties: System equivalence transformation," *IEEE Trans. Neural Netw. Learn. Syst.*, vol. 32, no. 9, pp. 3867–3879, Sep. 2021.

[10] M. Uchiyama, "Formation of high-speed motion pattern of a mechanical arm by trial," *Trans. Soc. Instrum. Control Eng.*, vol. 14, no. 6, pp. 706–712, 1978.

[11] S. Arimoto, S. Kawamura, and F. Miyazaki, "Bettering operation of robots by learning," *J. Robot. Syst.*, vol. 1, no. 2, pp. 123–140, 1984.

[12] M. Pierallini, F. Angelini, R. Mengacci, A. Palleschi, A. Bicchi, and M. Garabini, "Iterative learning control for compliant underactuated arms," *IEEE Trans. Syst. Man, Cybern. Syst.*, vol. 53, no. 6, pp. 3810–3822, Jun. 2023.

[13] D. Shen and J.-X. Xu, "An iterative learning control algorithm with gain adaptation for stochastic systems," *IEEE Trans. Autom. Control*, vol. 65, no. 3, pp. 1280–1287, Mar. 2020.

[14] R. Chi, H. Li, N. Lin, and B. Huang, "Data-driven indirect iterative learning control," *IEEE Trans. Cybern.*, vol. 54, no. 3, pp. 1650–1660, Mar. 2024.

[15] J. Chen and C. Hua, "Adaptive iterative learning fault-tolerant consensus control of multiagent systems under binary-valued communications," *IEEE Trans. Cybern.*, vol. 53, no. 11, pp. 6751–6760, Nov. 2023.

[16] Q. Wang, S. Jin, and Z. Hou, "Event-triggered cooperative model-free adaptive iterative learning control for multiple subway trains with actuator faults," *IEEE Trans. Cybern.*, vol. 53, no. 9, pp. 6041–6052, Sep. 2023.

[17] G. Liu and Z. Hou, "RBFNN-based adaptive iterative learning fault-tolerant control for subway trains with actuator faults and speed constraint," *IEEE Trans. Syst. Man, Cybern. Syst.*, vol. 51, no. 9, pp. 5785–5799, Sep. 2021.

[18] M. Sun, T. Wu, L. Chen, and G. Zhang, "Neural AILC for error tracking against arbitrary initial shifts," *IEEE Trans. Neural Netw. Learn. Syst.*, vol. 29, no. 7, pp. 2705–2716, Jul. 2018.

[19] Q. Yu, Z. Hou, X. Bu, and Q. Yu, "RBFNN-based data-driven predictive iterative learning control for nonaffine nonlinear systems," *IEEE Trans. Neural Netw. Learn. Syst.*, vol. 31, no. 4, pp. 1170–1182, Apr. 2020.

[20] W. Dong, J. A. Farrell, M. M. Polycarpou, V. Djapic, and M. Sharma, "Command filtered adaptive backstepping," *IEEE Trans. Control Syst. Technol.*, vol. 20, no. 3, pp. 566–580, May 2012.

[21] Z. Shao, Y. Wang, and X. Chen, "Global prescribed performance control for strict feedback systems pursuing uncertain target," *IEEE Trans. Neural Netw. Learn. Syst.*, vol. 35, no. 2, pp. 2403–2412, Feb. 2024.

[22] L. Liu, Y.-J. Liu, and S. Tong, "Neural networks-based adaptive finite-time fault-tolerant control for a class of strict-feedback switched nonlinear systems," *IEEE Trans. Cybern.*, vol. 49, no. 7, pp. 2536–2545, Jul. 2019.

[23] W. Li, X. Yao, and M. Krstic, "Adaptive-gain observer-based stabilization of stochastic strict-feedback systems with sensor uncertainty," *Automatica*, vol. 120, Oct. 2020, Art. no. 109112.

[24] S. Yin, P. Shi, and H. Yang, "Adaptive fuzzy control of strict-feedback nonlinear time-delay systems with unmodeled dynamics," *IEEE Trans. Cybern.*, vol. 46, no. 8, pp. 1926–1938, Aug. 2016.

[25] L. Sun, X. Huang, and Y. Song, "Distributed event-triggered control of networked strict-feedback systems via intermittent state feedback," *IEEE Trans. Autom. Control*, vol. 68, no. 8, pp. 5142–5149, Aug. 2023.

[26] B. Xu, Y. Shou, X. Wang, and P. Shi, "Finite-time composite learning control of strict-feedback nonlinear system using historical stack," *IEEE Trans. Cybern.*, vol. 53, no. 9, pp. 5777–5787, Sep. 2023.

[27] L. Li, K. Zhao, Y. Song, and F. L. Lewis, "On the uniformness of full-state error prescribed performance for strict-feedback systems," *IEEE Trans. Syst. Man, Cybern. Syst.*, vol. 54, no. 5, pp. 3022–3031, May 2024.

[28] L. Dugard and E. I. Verriest, *Stability and Control of Time-Delay Systems*. London, U.K.: Springer, 1998.

[29] Y. Chen, D. Huang, N. Qin, and Y. Zhang, "Adaptive iterative learning control for a class of nonlinear strict-feedback systems with unknown state delays," *IEEE Trans. Neural Netw. Learn. Syst.*, vol. 34, no. 9, pp. 6416–6427, Sep. 2023.

[30] X. Wu, J. H. Park, and M. Shen, "Adaptive iterative learning control for continuous systems with non-repetitive uncertainties and unknown state delays," *Int. J. Robust Nonlinear Control*, vol. 33, no. 4, pp. 2796–2810, Mar. 2023.

[31] J. Wei, Y. Hu, and M. Sun, "Adaptive iterative learning control for a class of nonlinear time-varying systems with unknown delays and input dead-zone," *IEEE/CAA J. Autom. Sinica*, vol. 1, no. 3, pp. 302–314, Jul. 2014.

[32] N. O. Perez-Arancibia, T.-C. Tsao, and J. S. Gibson, "Saturation-induced instability and its avoidance in adaptive control of hard disk drives," *IEEE Trans. Control Syst. Technol.*, vol. 18, no. 2, pp. 368–382, Mar. 2010.

[33] J.-X. Xu, Y. Tan, and T.-H. Lee, "Iterative learning control design based on composite energy function with input saturation," *Automatica*, vol. 40, no. 8, pp. 1371–1377, 2004.

[34] Z.-B. Wei, Q. Quan, and K.-Y. Cai, "Output feedback ILC for a class of nonminimum phase nonlinear systems with input saturation: An additive-state-decomposition-based method," *IEEE Trans. Autom. Control*, vol. 62, no. 1, pp. 502–508, Jan. 2017.

[35] G. Sebastian, Y. Tan, and D. Oetomo, "Convergence analysis of feedback-based iterative learning control with input saturation," *Automatica*, vol. 101, pp. 44–52, Mar. 2019.

[36] P. Pakshin, S. Mandra, J. Emelianova, E. Rogers, K. Erwiński, and K. Gałkowski, "Experimentally validated vector Lyapunov function-based iterative learning control design under input saturation," *IEEE Trans. Control Syst. Technol.*, vol. 32, no. 1, pp. 189–201, Jan. 2024.

[37] Q. Chen, H. Shi, and M. Sun, "Echo state network-based backstepping adaptive iterative learning control for strict-feedback systems: An error-tracking approach," *IEEE Trans. Cybern.*, vol. 50, no. 7, pp. 3009–3022, Jul. 2020.

[38] H. Chekireb, A. Boulkroune, and H. Benslimane, "Adaptive iterative learning control of nonlinearly parameterised strict feedback systems with input saturation," *Int. J. Autom. Control*, vol. 12, no. 2, p. 251, 2018.

[39] X. Bu, J. Liang, S. Wang, and W. Yu, "Robust guaranteed cost control for a class of nonlinear 2-D systems with input saturation," *Int. J. Control, Autom. Syst.*, vol. 18, no. 2, pp. 513–520, Feb. 2020.

[40] H. Li and Q. Wei, "Optimal synchronization control for multi-agent systems with input saturation: A nonzero-sum game," *Frontiers Inf. Technol. Electron. Eng.*, vol. 23, no. 7, pp. 1010–1019, Jul. 2022.

[41] H. Chu, J. Chen, Q. Wei, and W. Zhang, "Robust global consensus tracking of linear multi-agent systems with input saturation via scheduled low- and-high gain feedback," *IET Control Theory Appl.*, vol. 13, no. 1, pp. 69–77, Jan. 2019.

[42] L. Cao, X. Huang, H. Ye, and Y. Song, "Neuroadaptive asymptotic tracking control with guaranteed performance under mismatched uncertainties and saturated inputs," *IEEE Trans. Syst. Man, Cybern. Syst.*, vol. 53, no. 6, pp. 3784–3794, Jun. 2023.

[43] D. Shen and J. Xu, "Adaptive learning control for nonlinear systems with randomly varying iteration lengths," *IEEE Trans. Neural Netw. Learn. Syst.*, vol. 30, no. 4, pp. 1119–1132, Apr. 2019.

[44] J.-X. Xu and R. Yan, "On initial conditions in iterative learning control," *IEEE Trans. Autom. Control*, vol. 50, no. 9, pp. 1349–1354, Sep. 2005.

[45] S. Zhu, X. Wang, and H. Liu, "Observer-based iterative and repetitive learning control for a class of nonlinear systems," *IEEE/CAA J. Autom. Sinica*, vol. 5, no. 5, pp. 990–998, Sep. 2018.

[46] Q. Yu and Z. Hou, "Adaptive fuzzy iterative learning control for high-speed trains with both randomly varying operation lengths and system constraints," *IEEE Trans. Fuzzy Syst.*, vol. 29, no. 8, pp. 2408–2418, Aug. 2021.

[47] L. Xue, T. Zhang, W. Zhang, and X.-J. Xie, "Global adaptive stabilization and tracking control for high-order stochastic nonlinear systems with time-varying delays," *IEEE Trans. Autom. Control*, vol. 63, no. 9, pp. 2928–2943, Sep. 2018.